Continuum Methods 1

John Lowengrub

Dept Math
UC Irvine

Membranes, Cells, Tissues

- complex micro-structured soft matter

<u>Micro scale</u>

- Cell: ~10 micron
- Sub cell (genes, large proteins): nanometer

<u>Macro scale</u>

Tissues:
billion to 1000 billion cells
or
1—10 centimeter

Processes at cell scale

cell aggregation,
organ development

Signals at sub-cell scale

Outline

Give examples of continuum methods applied
to various problems in the four workshop areas:

- Membrane and protein science
- Microfluidics
- Angiogenesis and neovascularization
- Systems biology

Today:

- Biomembranes (1st talk)

- Microfluidics (2nd talk)

Focus: Different modeling approaches, advantages/disadvantages

Biomembranes

• main structural component complex architecture of biological systems

• Form interface between cell, and organelle structures with microenvironment

• Lipid bilayer containing cholesterol, proteins

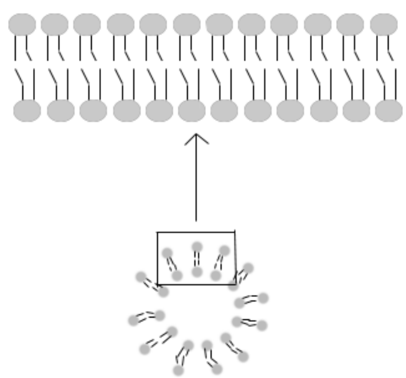

• Several nm thick, surface area can be several μm

•Can be highly mobile and fluid-like

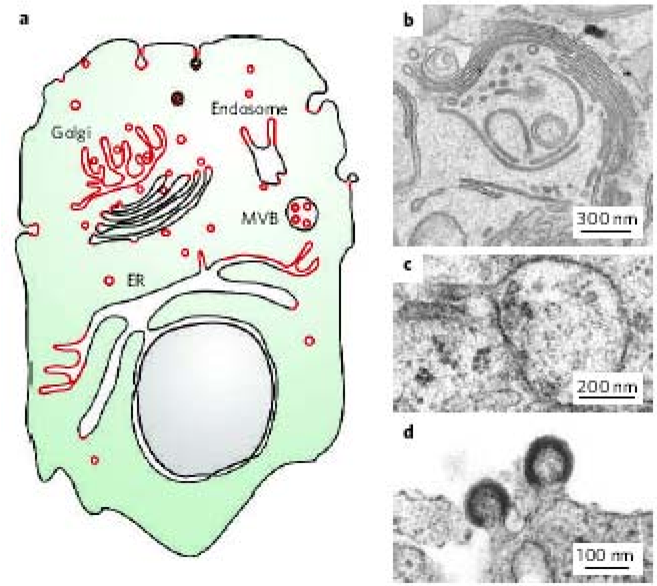

Figure 1 | Local differences in membrane curvature are hallmarks of cellular membranes. Many of the fine details of high local membrane curvature can be seen from the diagram (a) and the sample electron micrographs: b, fenestrations in the Golgi (from C. Hopkins and J. Burden, Imperial College London); c, tubule on endosomes (from P. Luzio and N. Bright, University of Utah); and d, HIV-1 viral budding (from W. Sundquist and U. von Schwedler, University of Utah). All of these can be described as local areas of positive or negative curvature (areas of high positive membrane curvature in a cell highlighted in red). Although it is fascinating to wonder how different membrane morphologies are adapted to the functions of different organelles, we concentrate here on how dynamic changes in morphology are generated. MVB, multi-vesicular body; ER, endoplasmic reticulum.

McMahon, Gallop. Nature 2005

• Membrane morphology changes during cellular movement, division and vesicle trafficking. Active role.

Biomembranes Contd.

- Membrane subdomains with particular curvature may have precise biological properties and function

Mechanisms to control membrane morphologies:

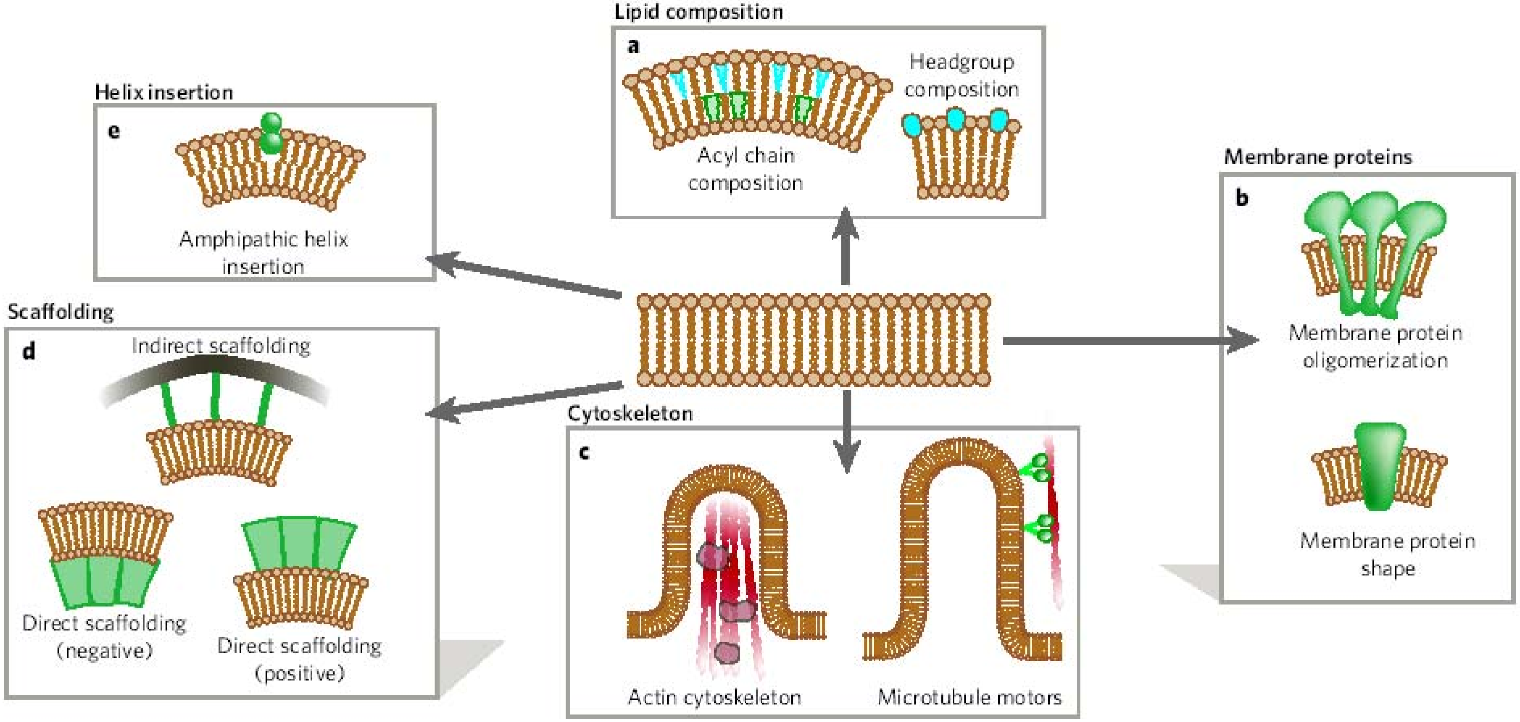

Figure 3 | Mechanisms of membrane deformation. The phospholipid bilayer can be deformed causing positive or negative membrane curvature. There are five main categories: **a**, changes in lipid composition; **b**, influence of integral membrane proteins that have intrinsic curvature or have curvature on oligomerization; **c**, changes in cytoskeletal polymerization and pulling of tubules by motor proteins; **d**, direct and indirect scaffolding of the bilayer; **e**, active amphipathic helix insertion into one leaflet of the bilayer.

McMahon, Gallop. Nature 2005

Mathematical Modeling

Bending energy/Spontaneous curvature model:

$$E = \int_{\Sigma} \tau + b_H \left(H - H_0\right)^2 + b_G G \, d\Sigma$$

surface energy

normal bending stiffness

spontaneous curvature

Gaussian bending stiffness

$H = (1/R_1 + 1/R_2)/2$ Mean curvature

$G = 1/(R_1 R_2)$ Gaussian curvature

Lipowsky, Nature 1991.

Constraints

- Area constraint

$$A = \int_{\Sigma} d\Sigma = A_0$$

(exchange of lipids with surrounding microenvironment is typically very slow)

- Volume constraint

$$Vol(\Sigma) = 1/3 \int_{\Sigma} \mathbf{x} \bullet \mathbf{n} \, d\Sigma = V_0$$

(limited osmosis, can be controlled however)

Morphology: Minimization of E subject to above constraints.

Related Problems

- Willmore flow
- Surface diffusion in materials
- Image processing

Willmore flow

$$E = \int_{\Sigma} H^2 \, d\Sigma$$

Normal velocity:

$$V = -\mu = -\frac{\delta E}{\delta \Sigma} = -\Delta_{\Sigma} H - 2H\left(H^2 - K\right)$$

•High order, nonlinear equation on moving boundary.

Germain, 1810
Willmore, *Riemannian Geometry* 1993.

Surface diffusion in materials

$$E = \int_{\Sigma} \tau(\mathbf{n}, H)\, d\Sigma$$

n Normal vector (reflects crystalline anistropy)

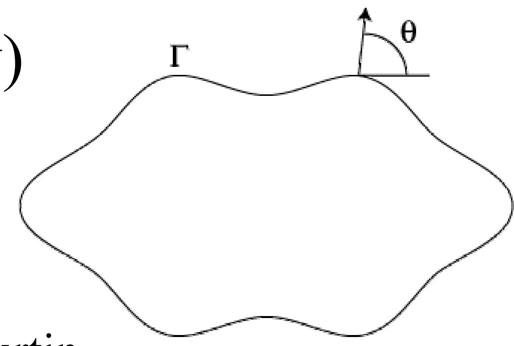

Example (2D): $\tau(\mathbf{n}, H) = \gamma(\theta) + \dfrac{\delta^2}{2} H^2$

DiCarlo, Gurtin, Podio-Duidugli, SIAM J. Appl. Math. (1992);Gurtin, Jabbour, Arch. Rat. Mech. Anal. (2002); Spencer, Phys. Rev. E (2004)

Then, chemical potential given by (2D)

$$\mu = \frac{\delta E}{\delta \Sigma} = -\left(\gamma(\theta) + \gamma''(\theta)\right) H + \delta^2 \left(H_{ss} + H^3\right)$$

Normal velocity: $V = \mu_{ss}$ → 6^{th} order system!

Wulff Shapes for 4-fold Anisotropy

$$\gamma(\theta) = 1 + a\cos(4\theta)$$

Wulff Shapes:

$\mu = const$

(given enclosed area)

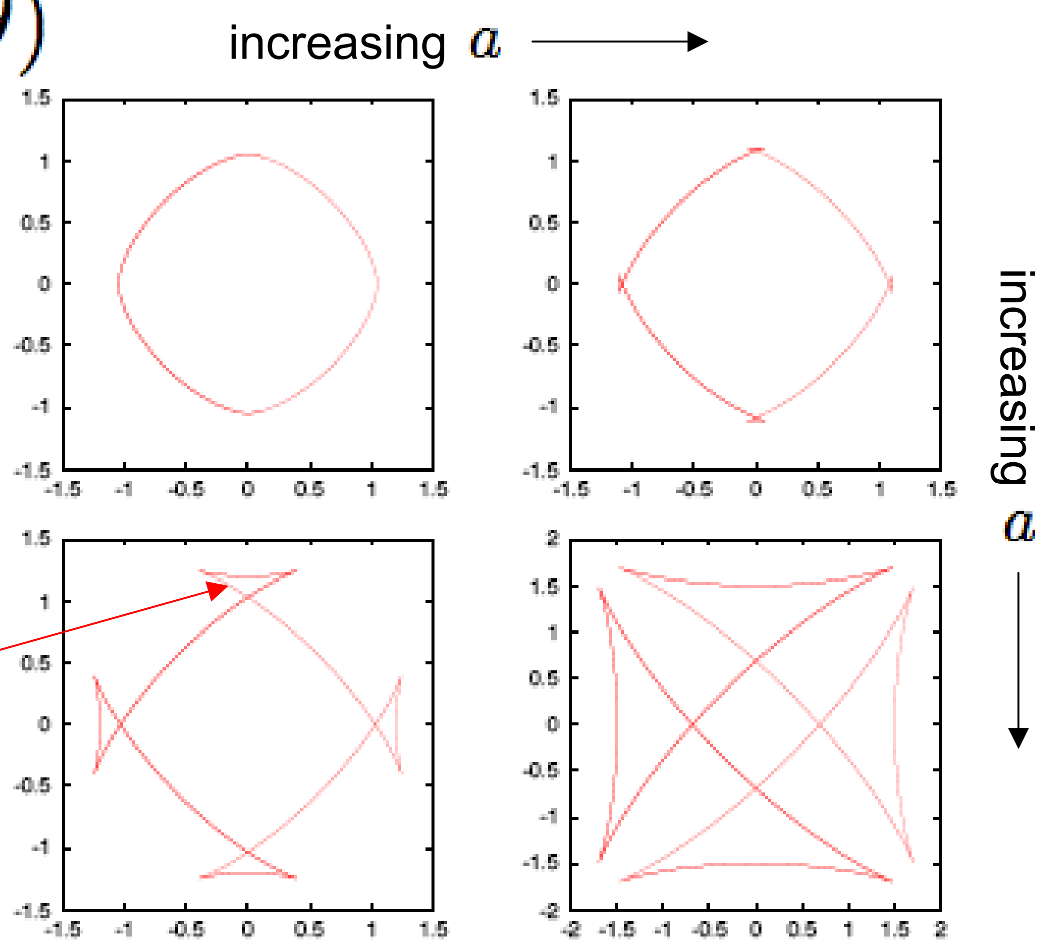

Nonphysical "ears" form for $a > 1/15$

Willmore regularization

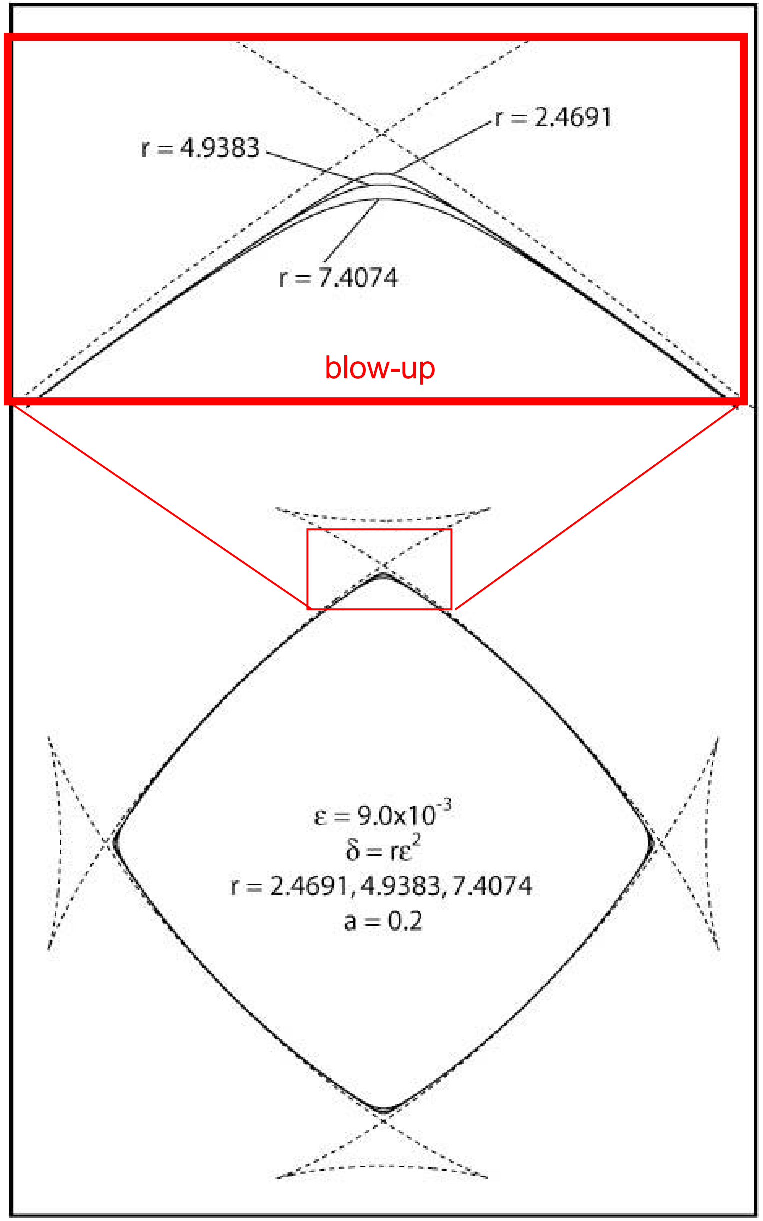

Willmore (α=1)

Image processing

Find a surface patch $\mathcal{M}$, such that $\widetilde{\mathcal{M}} := \mathcal{M} \cup \mathcal{M}^{ext}$ minimizes the Willmore energy

$$E[\mathcal{M}] := \frac{1}{2} \int_{\mathcal{M}} \mathbf{h}^2 \, \mathrm{d}x$$

over all C^1-surfaces $\widetilde{\mathcal{M}}$ with fixed exterior surface $\mathcal{M}^{ext}$.

Clarenz, et al, C. A. Geom. Design 2004

Xu, Pan, C.A.D. 2006

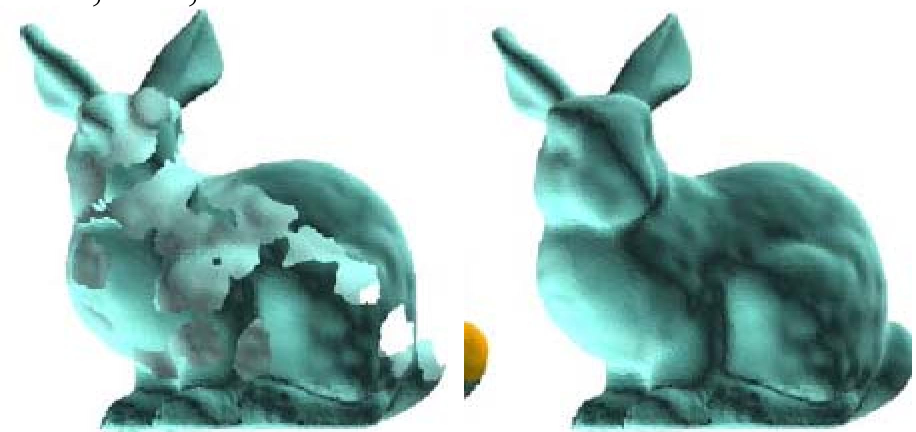

(a) (d)

ıows a bunny mesh with several co Shaded in different colors) and (d)
ɛ faired filler surfaces, after 2 itera s chosen to be 10^{-5}.

Fig. 3. Initial (top) and restored surface (bottom) of a venus head dataset from two different views. The areas of the surface to be restored are shown in darker grey. The time step was chosen as $\tau = 10^{-6}$, the restored surface corresponds to time $T = 20\tau$ and the grid size of the initial mesh varied between 0.0013 and 0.012. The initial object was scaled to diameter 1.

Difficulties

Numerical stiffness:

$$V \sim -\Delta_\Sigma H \longrightarrow \Delta t \leq \Delta s^4$$

•Surface diffusion $V = -\Delta_\Sigma H$ with Willmore regularization

$$V \sim \Delta_\Sigma^2 H$$

Computational Methods

•Sharp interface/front-tracking

•Level-set methods/front capturing

•Phase-field methods/front capturing

Sharp interface methods

- To overcome stiffness:

  Implicit discretizations, marker-point redistribution

Surface diffusion

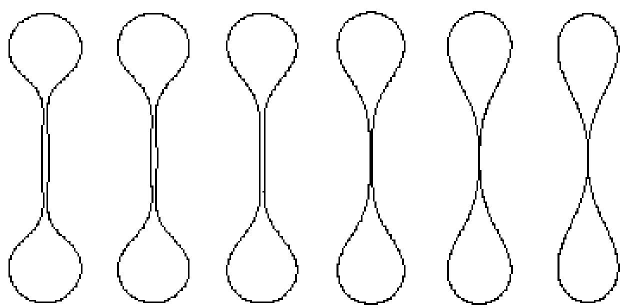

Fig. 2. Evolution of an embedded curve which self-intersects in finite time.

Bansch, Morin, Nochetto JCP 2005

Axisymmetric Willmore

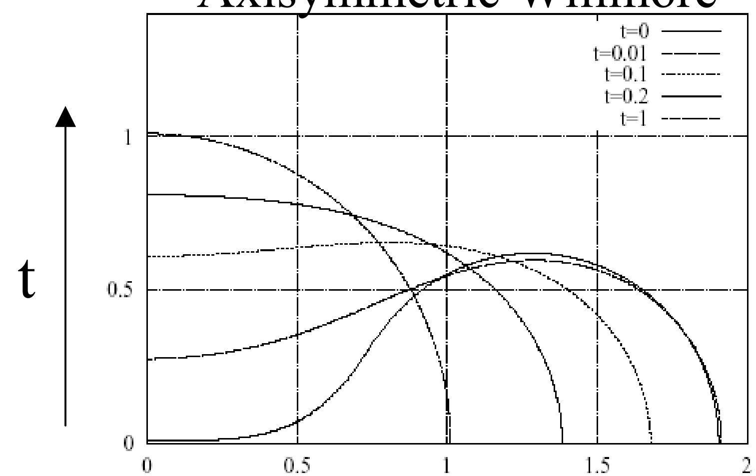

Figure 4: The generating curves of a dumbbell. Reflect the graphs in the y-axis and rotate about the x-axis for the full surface. A dumbbell does not pinch off under the Willmore flow, but evolves towards a sphere.

Mayer, Simonett. 2001

- Small scale decomposition (2D, Axisymmetric).

Hou, Lowengrub, Shelley JCP 1994

SSD for axisymmetric surfaces

$$\mathbf{x} = r\mathbf{r} + z\mathbf{z} \longrightarrow (r_t, z_t) = V\mathbf{n} + T\mathbf{s}$$

$$\mathbf{s} = (\cos\theta, \sin\theta)$$
$$\mathbf{n} = (\sin\theta, -\cos\theta)$$

Reformulation: θ and $s_\alpha = \sqrt{r_\alpha^2 + z_\alpha^2}$

$$\theta_t = -V_s + \theta_s T, \quad s_{\alpha,t} = (T_s + \theta_s V)\, s_\alpha$$

Total curvature $\quad 2H = \theta_s + \dfrac{\sin\theta}{r}$

Willmore flow/
Surface diffusion: $\quad V \sim -\theta_{sss}$

Dominant term at small spatial scales

Special choice of Tangential velocity

•Marker-points equally spaced in arclength: $s_\alpha = \int_0^1 s_{\alpha'} d\alpha' = L(t)$

$$\longrightarrow \quad T(\alpha,t) = T(0,t) - \int_0^\alpha V\theta_{\alpha'} d\alpha' + \alpha \int_0^1 V\theta_{\alpha'} d\alpha'$$

•Linear, constant coefficient equation at leading order:

$$\theta_t = -\frac{1}{L(t)^4}\theta_{ssss} + N(\alpha,t)$$

•Easy to apply implicit time integration algorithms

Extended form

Deviations from equal-arclength may arise. Can overcome by requiring instead:

$$\partial_t \left(s_\alpha - L(t) \right) = -\left(s_\alpha - L(t) \right)$$

This makes $s_\alpha = L(t)$ a stable manifold.

$$\longrightarrow \quad T(\alpha,t) = T(0,t) - \int_0^\alpha V\theta_{\alpha'} d\alpha' + \alpha \int_0^1 V\theta_{\alpha'} d\alpha' - \int_0^\alpha s_{\alpha'} d\alpha' + \alpha L(t)$$

additional terms

•Many other choices of tangential velocity possible.

(e.g., cluster points in regions of high curvature, etc.)

3D

Bansch, Morin, Nochetto JCP 2005.

Finite element approach. $V = -\Delta_S(\kappa + \varepsilon),$

Update: $\vec{X}^{n+1} = \vec{X}^n + \tau_n \vec{V}^{n+1}.$

Solve: $\vec{\kappa} = \Delta_S \vec{X}, \quad \kappa = \vec{\kappa} \cdot \vec{\nu}, \quad V = -\Delta_S(\kappa + \varepsilon), \quad \vec{V} = V\vec{\nu}.$

By:

$$
\begin{aligned}
&\vec{\kappa}^{n+1} - \tau_n \Delta_S \vec{V}^{n+1} = \Delta_S \vec{X}^n, \\
&\kappa^{n+1} - \vec{\kappa}^{n+1} \cdot \vec{\nu}^n = 0, \\
&V^{n+1} + \Delta_S \kappa^{n+1} = -\Delta_S \varepsilon^n, \\
&\vec{V}^{n+1} - V^{n+1} \vec{\nu}^n = 0.
\end{aligned}
$$

Δ_S: Evaluated on current (time n) surface

Using C0 elements.

Extension to Willmore flow
Burger, Voigt et al (2006)

3D Surface diffusion

Mesh adaptivity using *a posteriori* error estimates

Implementation using Albert

Schmidt, Sieberg, Acta Math. 2000

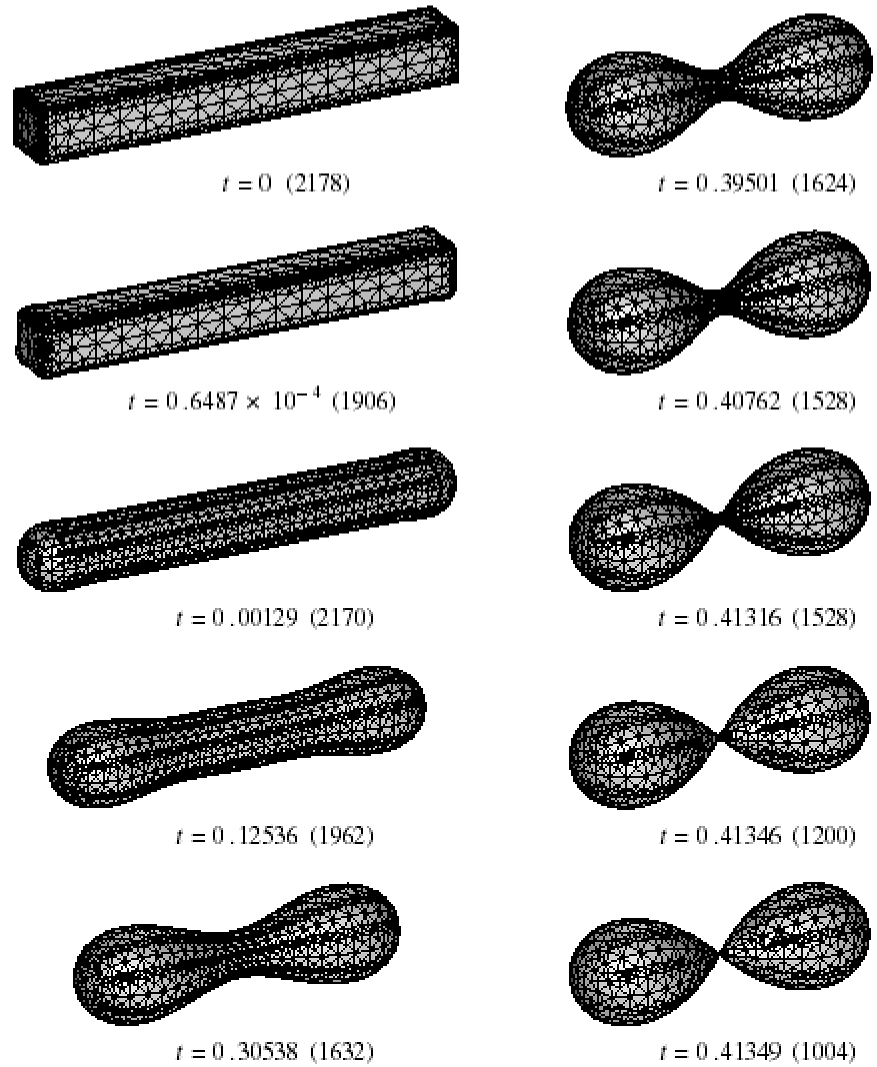

•Leads to topology change

Bansch, Morin, Nochetto JCP 2005.

Level-set methods

Osher, Sethian 1988

•Interface capturing.

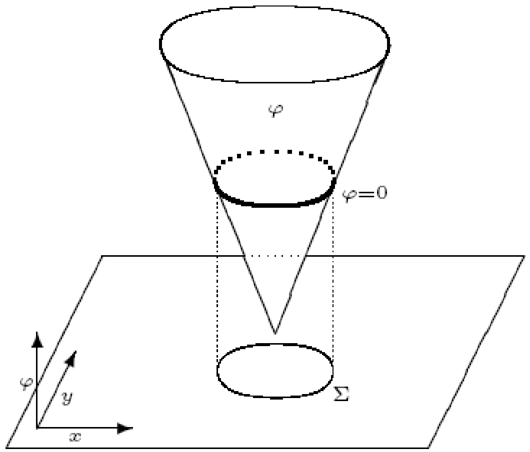

$$\Sigma(t) = \{\mathbf{x} \mid \phi(\mathbf{x},t) = 0\}$$

•Interface moves with speed *V*:

$$\phi_t + V_{ext} \mid \nabla \phi \mid = 0 \quad \text{where } V_{ext} \text{ is an extension of } V \text{ off } \Sigma$$

Willmore flow.

Droske, Rumpf
IFB 2004

Given an initial function ϕ_0 on Ω find a pair of functions (ϕ, w) with $\phi(0) = \phi_0$, such that

$$\int_\Omega \frac{\partial_t \phi}{\|\nabla \phi\|} \vartheta \, dx = \int_\Omega -\frac{1}{2} \frac{w^2}{\|\nabla \phi\|^3} \nabla \phi \cdot \nabla \vartheta - \|\nabla \phi\|^{-1} P \nabla w \cdot \nabla \vartheta \, dx \,, \quad (9)$$

$$\int_\Omega \|\nabla \phi\|^{-1} w \, \psi \, dx = \int_\Omega \frac{\nabla \phi}{\|\nabla \phi\|} \cdot \nabla \psi \, dx \quad (10)$$

$$w := -\|\nabla \phi\| \; h$$

weighted mean curvature

for all $t > 0$ and all functions $\vartheta, \psi \in C_0^\infty(\Omega)$.

•Semi-implicit discretization

Level-set results (sample)

Willmore flow

Droske, Rumpf
IFB 2004

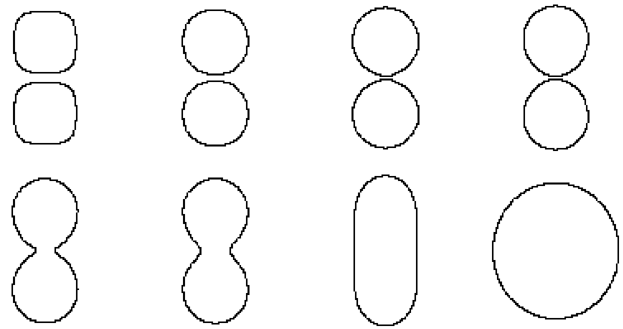

Figure 6: Two shapes merge under the level set evolution of Willmore flow. The parameters were chosen as follows: $\epsilon = 5h$, where $h = 128^{-1}$, the time step size τ was $10h^4$. Timesteps $0, 100, 800, 1600, 1700, 1800, 4000, 40000$ are depicted from top left to bottom right.

Anisotropic surface diffusion with Willmore regularization

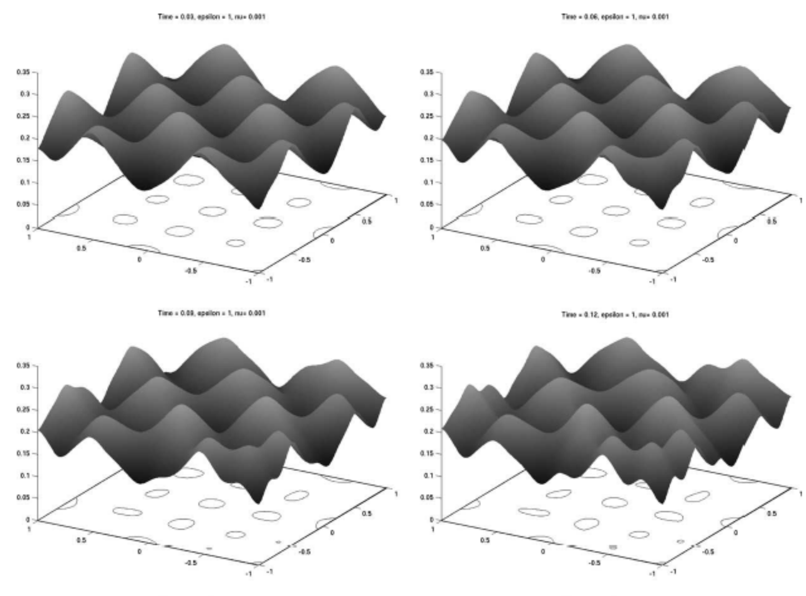

Burger, JCP 2005.

Phase-field methods

c is a smooth order parameter

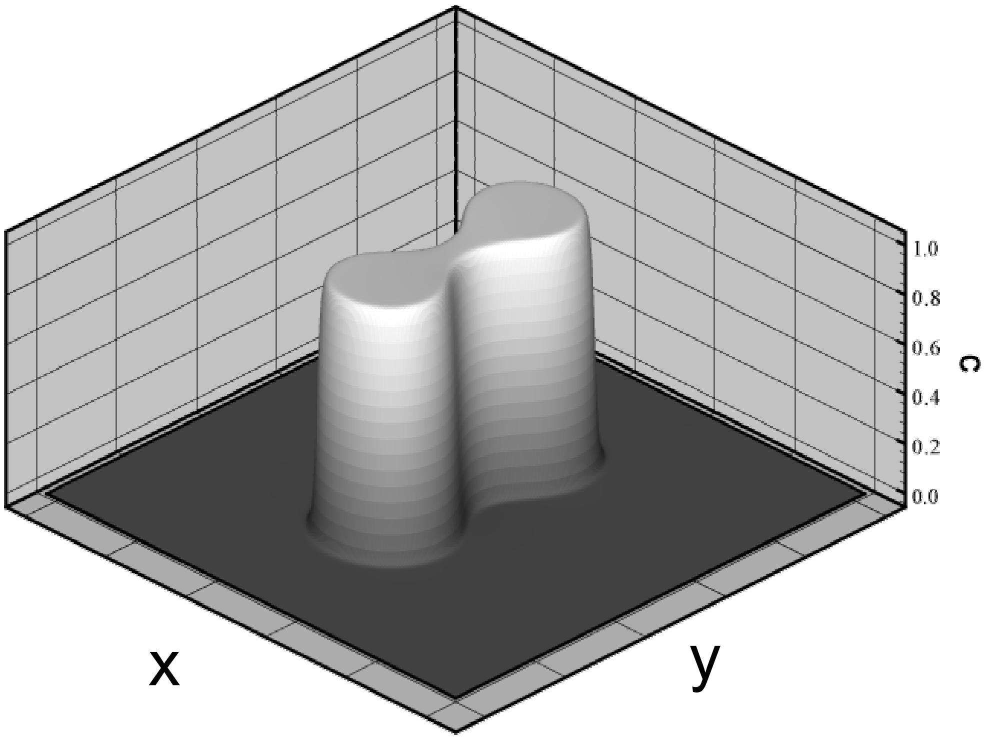

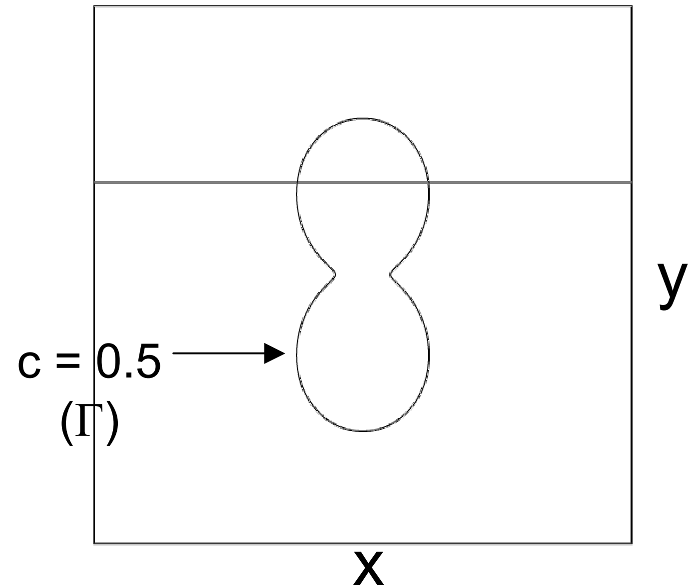

y=const cross-section

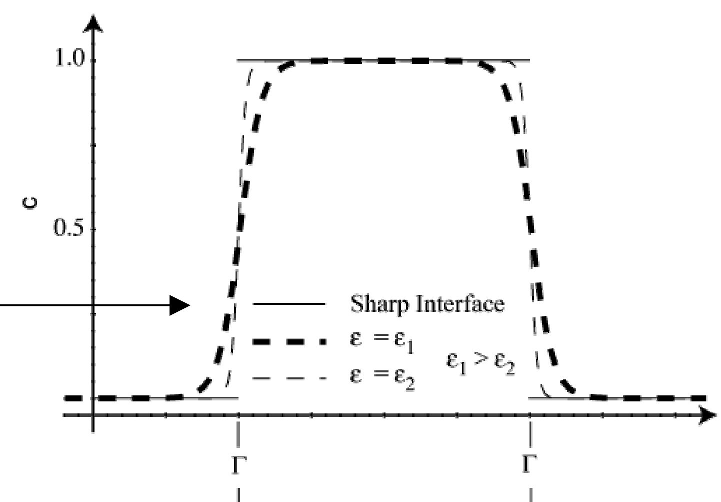

Why Phase-field?

- Allows the easy capture of interface dynamics.
- Avoid explicit tracking.
- Easy to add more physics (e.g., elasticity, multiple phases).
- Downside: introduce finite thickness.

diffuse interface

Phase-field Willmore Problem

$$\mathcal{E}_{W,\epsilon} = \int_\Omega \frac{\epsilon}{2} \left(\Delta c - \frac{1}{\epsilon^2} F'(c) \right)^2 \, d\mathbf{x}$$

Du *et al.* showed rigorous asymptotic convergence ($\epsilon \to 0$) of solutions of

$$\frac{\delta \mathcal{E}_{W,\epsilon}}{\delta c} = 0$$

to solutions of the classical Willmore problem

$$\mathcal{E}_W = \int_\Gamma H^2 \, ds$$

$$\frac{\delta \mathcal{E}_W}{\delta \Gamma} = \Delta_\Gamma H + 2H(H^2 - K) = 0$$

Qiang Du *et al*, *A phase field formulation of the Willmore problem,* Nonlinearity (2005).

Evolution equations

Gradient flow approach:

$$\frac{\delta E_{W,\varepsilon}}{\delta c} = \mu = \frac{1}{\varepsilon^3}\left(\nu F''(c) - \varepsilon^2 \Delta \nu\right),$$

$$\nu = F'(c) - \varepsilon^2 \Delta c$$

Phase field equation:

$$c_t = -\mu = -\frac{1}{\varepsilon^3}\left(\nu F''(c) - \varepsilon^2 \Delta \nu\right),$$

$$\nu = F'(c) - \varepsilon^2 \Delta c$$

4th order nonlinear equation. (non conserved)

3D Anisotropic Diffuse Interface Model

order parameter $0 \le c \le 1$ finite interfacial thickness corner rounding

$$\mathcal{E} = \int_\Omega \left(F(c) + \frac{\epsilon^2}{2} |\gamma(\mathbf{n}) \nabla c|^2 + \frac{\delta^2}{2} \left(\Delta c - \frac{\alpha}{\epsilon^2} F'(c) \right)^2 \right) d\mathbf{x}$$

double well energy density anisotropy asymptotically like H^2 for α=1

- (α=0) Wise, Lowengrub, Kim, Thornton, Voorhees, Johnson, Appl. Phys. Lett. (2005)
- (α=1) Ratz, Ribalta, Voigt, J. Comput. Phys. (2005)
- (α=0,1) Kim, Wise, Lowengrub (in preparation)

Evolution: 6th-order Cahn-Hilliard Eqn

mass conservation:
M = 1, bulk diff.; M = c(1-c), surface diff.

diagonal anisotropy matrix

$$
\begin{aligned}
\frac{\partial c}{\partial t} &= \nabla \cdot (M(c)\nabla \mu) \\
\frac{\delta \mathcal{E}}{\delta c} =: \mu &= (1-\alpha)F'(c) - \left(\epsilon^2 + \alpha \frac{\delta^2}{\epsilon^2} F''(c)\right)\nu - \nabla \cdot (\mathcal{A}(\mathbf{n})\nabla c) + \delta^2 \Delta \nu \\
\nu &= \Delta c - \frac{\alpha}{\epsilon^2} F'(c)
\end{aligned}
$$

linear biharmonic for $\alpha = 0$

Asymptotic convergence to the sharp interface surface diffusion model?

Discretization of Cahn-Hilliard Eq.: α=0 case

Crank-Nicholson

$$
\begin{aligned}
\frac{c_{ij}^{n+1} - c_{ij}^{n}}{s} &= \frac{1}{2}\left[\nabla_d \cdot \left(M(c_{i,j}^{n+1})\nabla_d \mu_{ij}^{n+1}\right) + \nabla_d \cdot \left(M(c_{i,j}^{n})\nabla_d \mu_{ij}^{n}\right)\right] \\
\mu_{ij}^{n+1} &= f(c_{ij}^{n+1}) - \epsilon_0^2 \nu_{ij}^{n+1} - \nabla_d \cdot \left(\mathcal{A}(\mathbf{n}_{i,j}^{n+1})\nabla c_{i,j}^{n+1}\right) + \delta^2 \Delta_d \nu_{ij}^{n+1} \\
\nu_{ij}^{n+1} &= \Delta_d c_{ij}^{n+1}
\end{aligned}
$$

center-differencing (compact stencils)

Solve nonlinear elliptic problem using adaptive full approximation scheme (AFAS) for each time step n.

Linearizations

local Picard-linearization: GS

$$
\begin{aligned}
\frac{c_{ij}^{n+1} - c_{ij}^{n}}{s} &= \frac{1}{2}\left[\nabla_d \cdot \left(M(c_{i,j}^{n+1})\nabla_d \mu_{ij}^{n+1}\right) + \nabla_d \cdot \left(M(c_{i,j}^{n})\nabla_d \mu_{ij}^{n}\right)\right] \\
\mu_{ij}^{n+1} &= f(c_{ij}^{n+1}) - \epsilon_0^2 \nu_{ij}^{n+1} - \nabla_d \cdot \left(\mathcal{A}(\mathbf{n}_{i,j}^{n+1})\nabla c_{i,j}^{n+1}\right) + \delta^2 \Delta_d \nu_{ij}^{n+1} \\
\nu_{ij}^{n+1} &= \Delta_d c_{ij}^{n+1}
\end{aligned}
$$

local Newton-linearization: GS

local Picard-linearization: Vcycle

anisotropy is fully implicit!

Details

- Mild solvability time-step restriction (being remedied)
- No time-step restriction owing to anisotropy
- Tests indicate 2nd order accuracy method (c, *a posteriori in* l_2)

•J.S. Kim, K. Kang, and J.S. Lowengrub, *Conservative multigrid methods for Cahn-Hilliard fluids*, J. Comput. Phys., (2004)
•Wise et al., Appl. Phys. Lett. (2005) (QD self assembly)

•Kim, Wise, Lowengrub, *Adaptive Method for Strong Anisotropy* (in preparation)

Isotropic Spinodal Decomposition (a=0, δ=0)

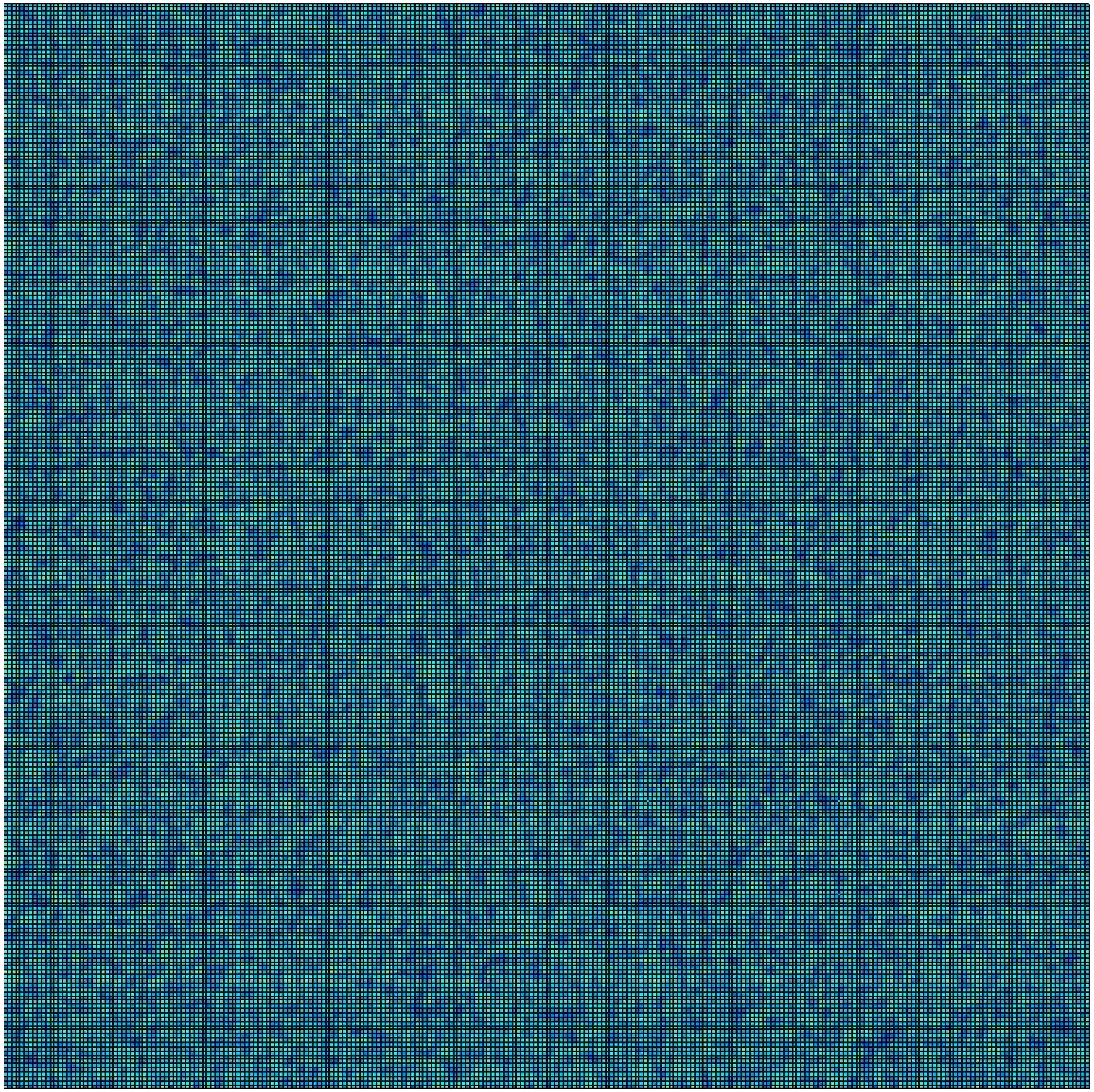

30% volume fraction

- base level = 64^2
- 2 levels of refinement
- effective 256^2

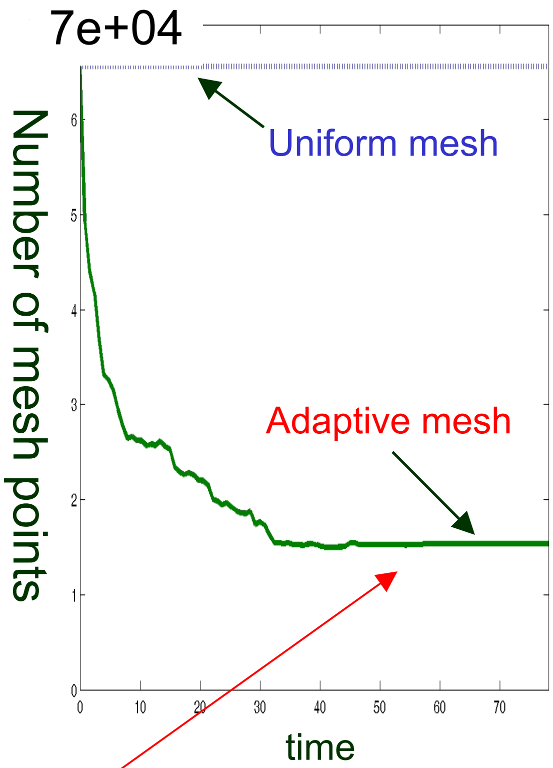

1/6 cost (long times)

2D Mesh: 2 Levels of Refinement

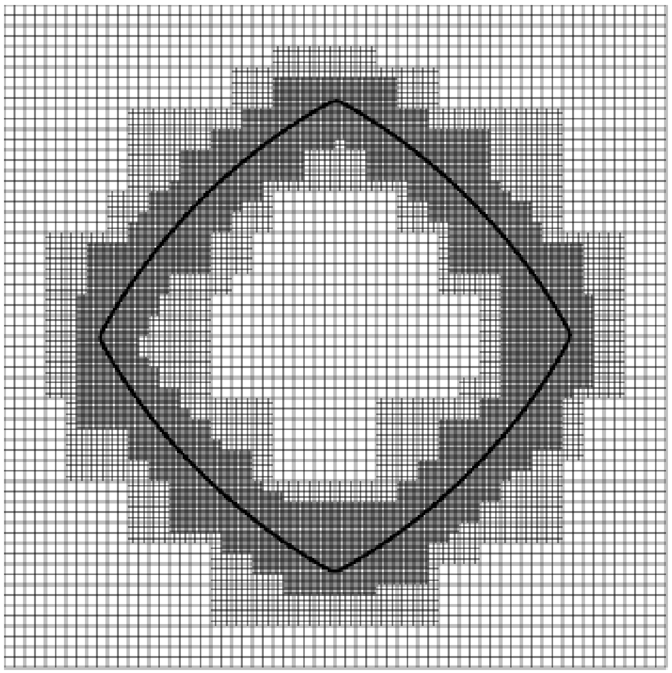

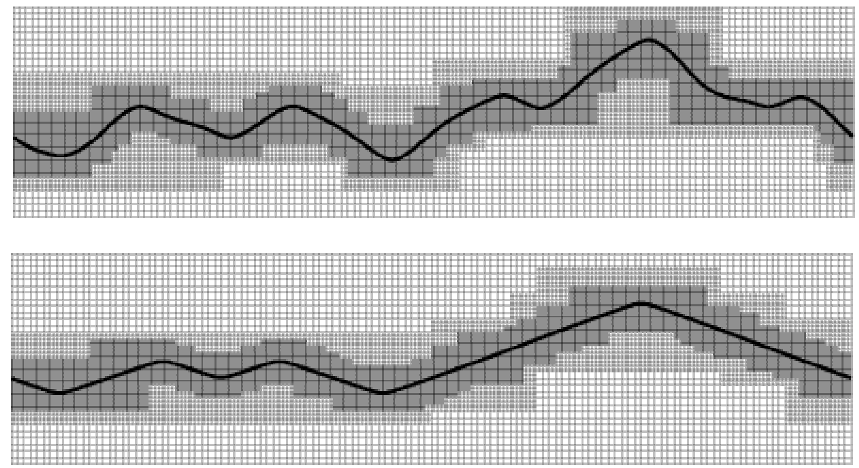

Kim, Wise, Lowengrub, (in preparation).

3D Adaptive Computations

interface thickness

corner rounding

4-fold anisotropy

- $\varepsilon = 1.8\text{e-}02$, $\delta = 5.0\text{e-}04$, $a = 0.2$

$h_2 \sim \varepsilon$

- base grid 32^3, 2 levels, $h_2 = 3.2/128$
- surface diffusion, $M = c(1-c)$
- $c = 0.5$ isosurfaces

Anisotropic surface energy + Willmore regularization

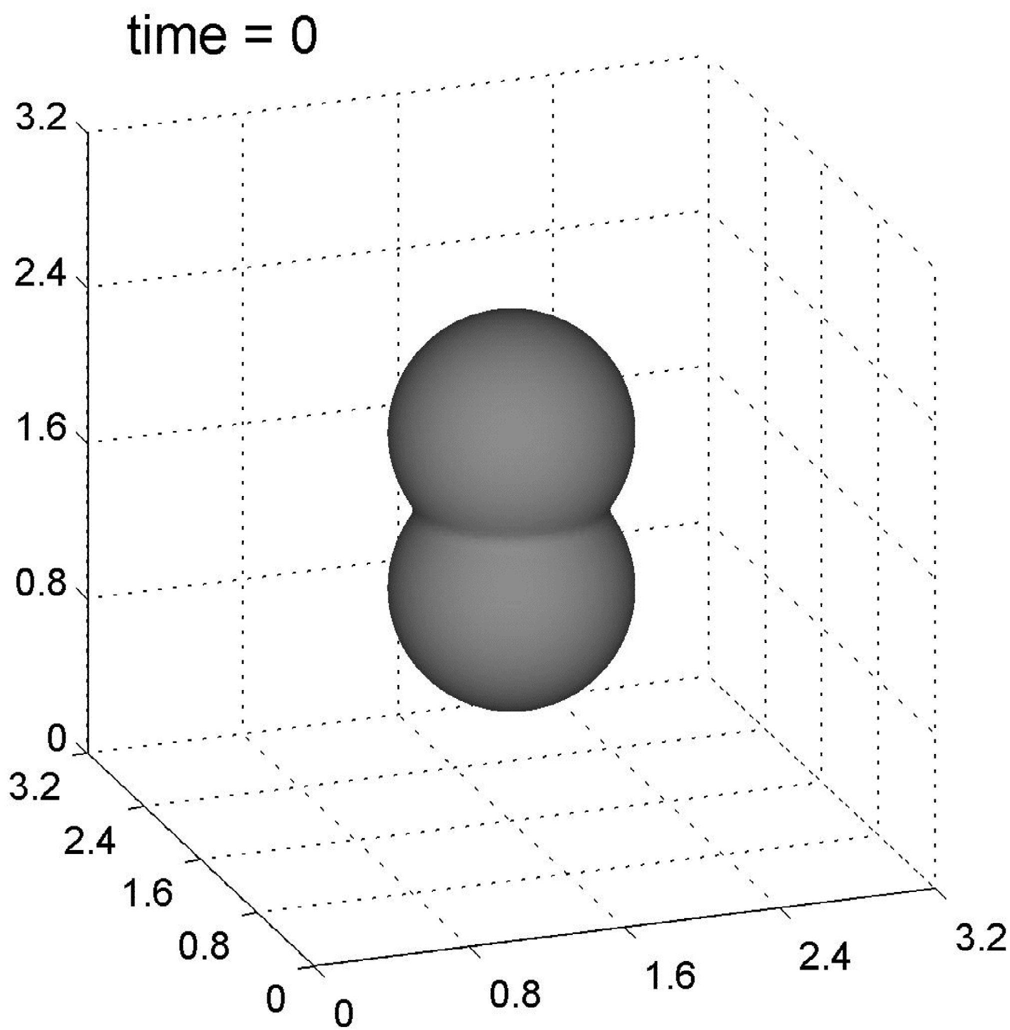

- Evolution to Wulff shape

Adaptive Mesh

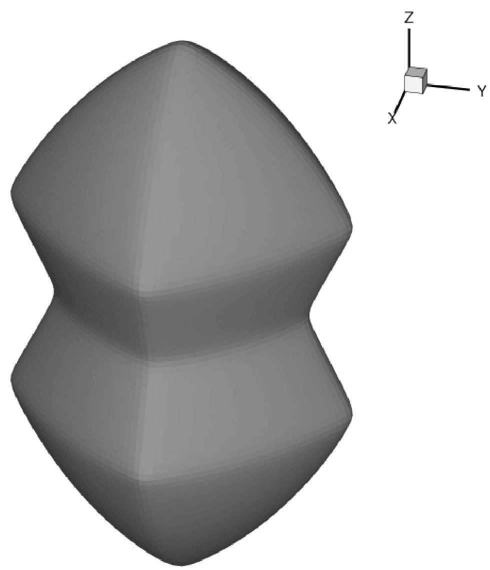

t = 4.0
(magnified view)

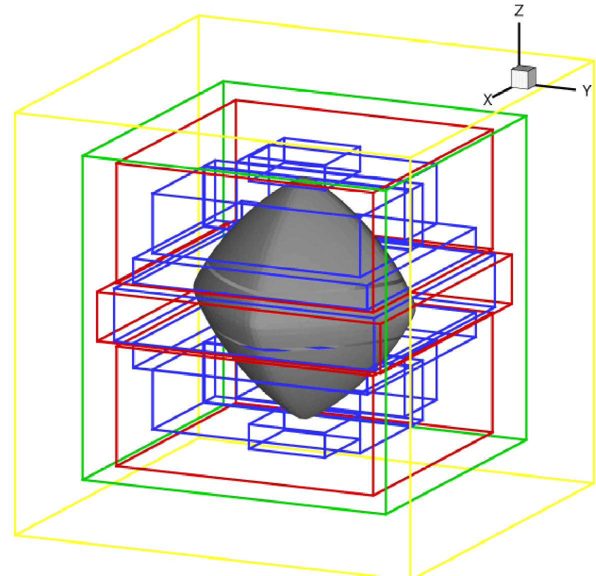

t = 20.0 (with mesh)

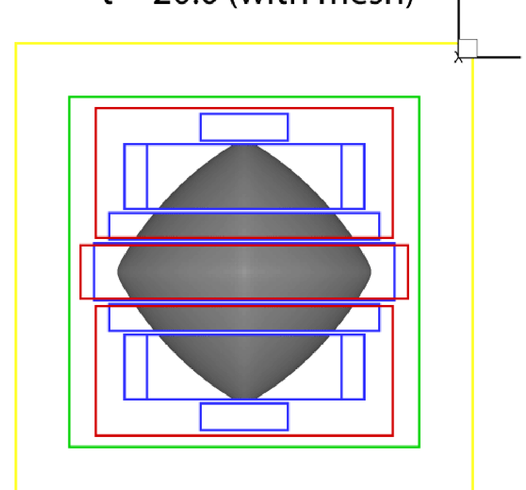

Phase-field formulation of membrane problem

Du, Liu, Wang JCP 2004 and 2006.

$$W(\phi) = \int_\Omega \frac{k\epsilon}{2} \left| \Delta\phi - \frac{1}{\epsilon^2}(\phi^2 - 1)(\phi + C\epsilon) \right|^2 \mathrm{d}x,$$ Bending energy

$$A(\phi) = \int_\Omega \phi(x)\, \mathrm{d}x,$$ volume

$$B(\phi) = \int_\Omega \left[\frac{\epsilon}{2} |\nabla\phi|^2 + \frac{1}{4\epsilon}(\phi^2 - 1)^2 \right] \mathrm{d}x.$$ Surface area

Gradient flow:

$$\phi_t = -\gamma \frac{\delta W}{\delta\phi} + \lambda_1 \frac{\delta A}{\delta\phi} - \lambda_2 \frac{\delta B}{\delta\phi}.$$

λ_1, λ_2 Lagrange multipliers for volume and area conservation.

Numerical methods

•Implicit time discretization,

•Discrete energy law,

•Periodic BC, pseudo-spectral methods

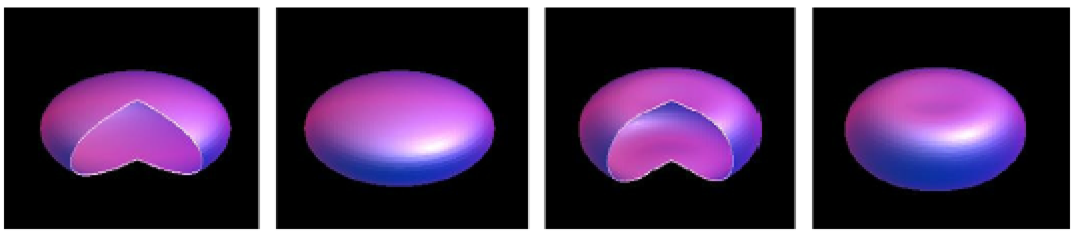

•Evolution to a discocyte

•Evolution to a torus

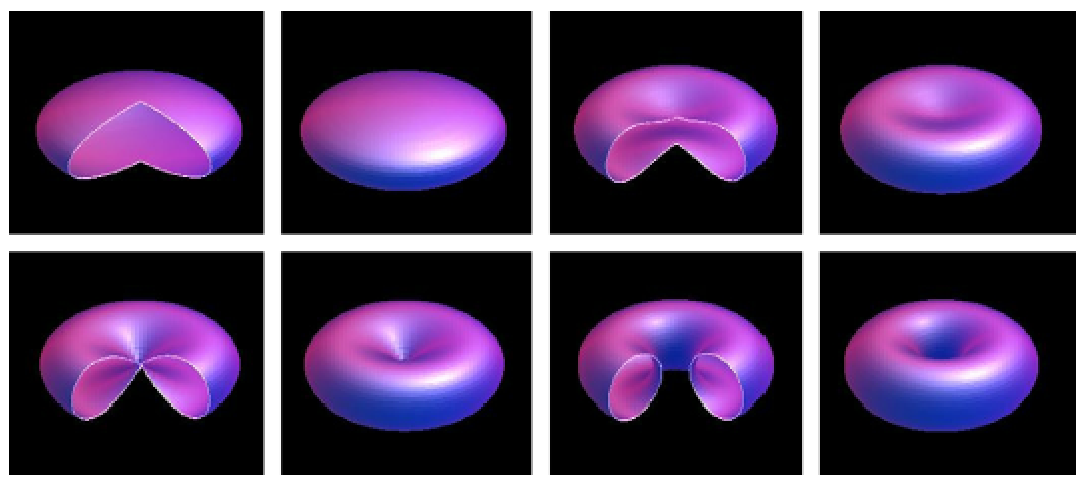

Fig. 7. A flat ellipsoid shaped vesicle pinches off to a torus.

Du, Liu, Wang
JCP 2006

Further directions

- Effects of fluid flow

  Du et al. for single-component membranes (to appear)
  Lowengrub et al for multicomponent membranes
  (in progress)

- Multicomponent membranes

  More than one lipid component

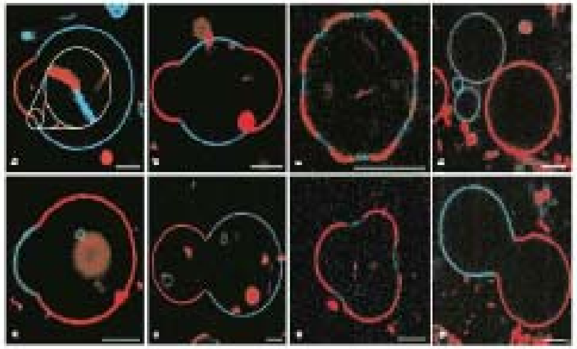

Baumgart, Hess, Webb
Nature 2003

Du et al., phase-field models
Lowengrub, Voigt et al., sharp interface models